

# Subject Position Affects EEG Magnitudes

Justin K. Rice<sup>a</sup>, Christopher Rorden<sup>b</sup>, Jessica S. Little<sup>c</sup>, Lucas C. Parra<sup>a,1</sup>

<sup>a</sup>*City College of the City University of New York, Room ST-403, 160 Convent Avenue, New York, NY, 10031*

<sup>b</sup>*University of South Carolina, 915 Greene Street, Columbia, SC 29208*

<sup>c</sup>*University of North Carolina, Chapel Hill, NC 27599*

---

## Abstract

EEG (electroencephalography) has been used for decades in thousands of research studies and is today a routine clinical tool despite the small magnitude of measured scalp potentials. It is widely accepted that the currents originating in the brain are strongly influenced by the high resistivity of skull bone, but it is less well known that the thin layer of CSF (cerebrospinal fluid) has perhaps an even more important effect on EEG scalp magnitude by spatially blurring the signals. Here it is shown that brain shift and the resulting small changes in CSF layer thickness, induced by changing the subject's position, have a significant effect on EEG signal magnitudes in several standard visual paradigms. For spatially incoherent high-frequency activity the effect produced by switching from prone to supine can be dramatic, increasing occipital signal power by several times for some subjects (on average 80%). MRI measurements showed that the occipital CSF layer between the brain and skull decreases by approximately 30% in thickness when a subject moves from prone to supine position. A multiple dipole model demonstrated that this can indeed lead to occipital EEG signal power increases in the same direction and order of magnitude as those observed here. These results suggest that future EEG studies should control for subjects' posture, and that some studies may consider placing their subjects into the most favorable position for the experiment. These findings also imply that special consideration should be given to EEG measurements from subjects with brain atrophy due to normal aging or neurodegenerative diseases, since the resulting increase in CSF layer thickness could profoundly decrease scalp potential measurements.

*Keywords:* EEG, Current Source Modeling, Neuroanatomy, Gamma Power, ERP Magnitude, Brain Shift

---

## 1. Introduction

Electroencephalography (EEG) is one of the oldest sensor modalities in neurology and neuroscience, and is still frequently used in both the clinic and the lab. It continues to increase scientific understanding of brain function and functional localization, and in the clinic it is used diagnostically for epilepsy and other diseases and as a monitor during many procedures and surgeries [40][44][52][23]. EEG signals are also used as an index for alertness, attention, and inhibition, and are the most common "interface" in brain-computer-interfaces (BCIs, or brain-machine interfaces-BMIs) [25][12][31][27]. So important is this modality to all manner of physiological, cognitive science, and neurological research that the effects of a plethora of factors on EEG have been investigated. A quick literature search will find studies on the effect on EEG of various pharmaceuticals, temperature, music, mood, lighting, aromatherapy, and meditation, just to name a few.

The prominence of EEG in neuroscience methods, along with its low signal-to-noise ratio, have prompted many investigations into methods for maximizing information extraction e.g. [16][5][54][48], often using advanced signal processing and classification algorithms, and it is standard practice in research to use an expensive shielded room as a Faraday cage [46] to minimize

---

<sup>1</sup>To whom correspondence should be addressed: E-mail parra@ccny.cuny.edu

noise. Yet relatively little research has been done on the effects of subject head orientation, relative to gravity, on the EEG signal. The literature that does exist mostly focuses on the effect of baroreception on sitting vs. supine positions (see [26] for a review).

Recent papers have shown that the force of gravity may cause the brain to shift between prone and supine positions [49], due to its negative buoyancy in cerebro-spinal-fluid (CSF) [34]. While minor in comparison to the thickness of the skin and skull, not to mention the resolution of EEG electrodes, the conductivity of CSF is 50-100 times that of the skull and fat, and 5-10 times that of gray matter [35]. This gives its distribution a potentially much larger effect on the measured scalp voltage potentials, as shown in [39][38][51] where the effect of neglecting CSF thickness is investigated using realistic head models. This is especially true for signals with non-spatially-coherent sources, e.g. gamma activity [17], wherein the CSF ‘smears’ the neighboring signals together [37][14], resulting in a cancelling effect, adding to the more obvious effect produced simply by moving the brain closer or farther from the electrodes. Hence, it is hypothesized that this 30-50% change in the total thickness of the CSF from prone to supine positions will have a large effect on the EEG signal.

In this paper the effects of subject position on EEG signals are measured in the occipital cortex. MRI data from prone and supine positions supported literature estimates of a significant change in CSF thickness in this region. Monte-Carlo simulations of multiple dipoles in a spherical head model estimated that this change in CSF thickness would produce large increases in occipital signal power, which matched the direction and order of magnitude of the empirical EEG results. These large changes in signal strength suggest that subject position is an important consideration in BCI experiments, general EEG-based research, and clinical usage.

## 2. Materials and Methods

### 2.1. MRI Experiment and Data Analysis

T1-weighted MRI scans (3D MP-RAGE sequence, TR=2250ms, TI=900ms, TE=4.52, 9-degree flip angle with 176 1mm sagittal slices, each with a  $256 \times 256$  matrix and  $256 \times 256$  mm FOV), eight prone, and nine supine (eight for analysis, one for coregistration), were performed on three male subjects (authors CR, JKR, LCP) using a Siemens Trio 3.0 Tesla MRI system fitted with a twelve-channel headcoil. Scans were acquired in a counterbalanced order. Between images the participant was always asked to get out of the scanner and stand up prior to being repositioned for the next scan, even if the posture was repeated between a pair of scans. This ensured that the head position and scanner shim would have similar variability between postures and within postures.

All scans were segmented using SPM8’s new segment procedure [2] and then coregistered using SPM8’s DARTEL normalization [1], and the results were used to create supine and prone statistical parametric models (SPMs) using SPM8. The % composition of CSF in voxels in the frontal and occipital regions were then each integrated along the anterior-posterior axis to find an estimate of the CSF thickness, where the domain of integration is either the frontmost or rearmost regions of cortex, in this case being the anterior-most 3.3cm and posterior-most 3.0cm of the head (limited by encroachment of the cerebellum, eyes, ventricles, etc.). The resulting estimates of CSF thickness, can be compared between the prone and supine positions to find the relative change (see Fig. 1). However, in general these are projections of the CSF thickness change onto the coronal plane. For the statistical test, we limit the analysis to areas where the skull was orthogonal to the anterior-posterior axis but excluding the projection of the falx cerebri, - thus giving unbiased estimates of the CSF thickness change in these regions. Unpaired t-tests were then performed on the average over these restricted regions of the eight prone and eight supine images.

### 2.2. Spherical Head-modeling and Multi-Dipole Simulations

To investigate conceptually whether or not small CSF thickness changes can account for EEG signal strength changes of the direction and order of magnitude observed here, a heterogeneous concentric sphere model was developed. Five dipoles were modeled at 7.5-degree intervals (about

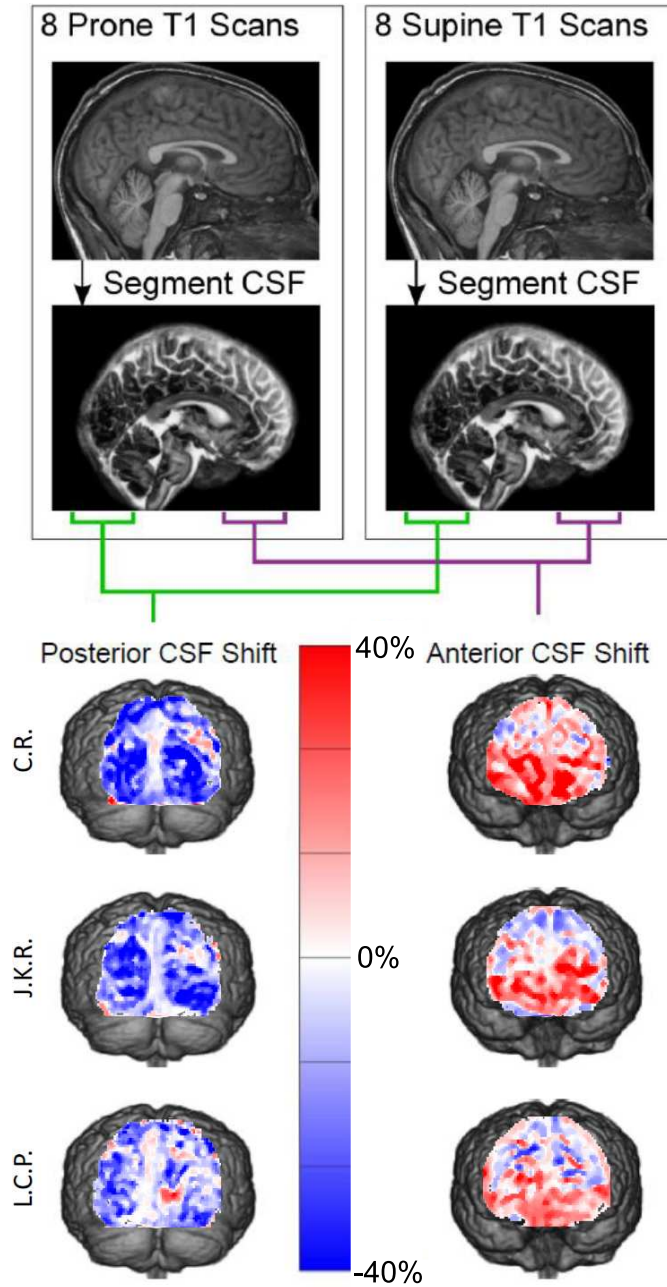


Figure 1: Conceptual diagram of MRI data collection and analysis. Colored plots (overlaid on corresponding cortical surface) represent % change in CSF thickness (coronal projection) from prone to supine positions )

1cm on the cortical surface), placed 1mm beneath the surface of the cortex. Because of the linearity of the Poisson equation, one can simply add up the potential contributions of multiple dipoles, each using equation 1 (see Appendix). Each dipole was assigned a random phase at 55Hz, and simulated to oscillate for 5 seconds, while the corresponding potentials were calculated on the scalp at 5-degree intervals. This was done 100 times for both axially and tangentially oriented dipoles, and for CSF thicknesses of 2mm and 3mm. The spectral estimates were then calculated using the same procedure and tools used for the EEG data (below), and averaged over trials. Conductances were taken from [22] and sphere radii from [57] (the radius of the grey matter was 6.3cm, the skull and scalp thicknesses were 6mm and 4mm respectively, and the CSF was modeled as either 2mm or 3mm thick). The conductances were  $\rho_{brain} = 300\Omega cm$ ,  $\rho_{CSF} = 65\Omega cm$ ,  $\rho_{skull} = 5000\Omega cm$ ,  $\rho_{scalp} = 65\Omega cm$ , giving a CSF:skull ratio of approximately 1:77. See the appendix for a derivation of the four-region volume conduction model.

To investigate what proportion of the effect were due to the high conductivity of the CSF itself, and what portion could be accounted for by the effect of simply moving the brain relatively closer to the electrodes, the above simulations were also conducted using a model wherein the CSF was given the same conductance as the gray matter.

### 2.3. Point Spread Function

In order to compare the localization of scalp potentials of dipoles under certain conditions, the proportion of global power in a 15 degree radius can be calculated. Integrating over the local surface  $\mathcal{D}_{local}$  (15 degrees in  $\theta$ , represented by  $\mathcal{D}_{\theta_{local}}$ ) of highest potential and normalizing by the integral over the entire surface,  $\mathcal{D}_t$  :

$$P_{local} = \frac{\int_{\mathcal{D}_{local}} V(r_s, \theta, \beta)^2 dS}{\int_{\mathcal{D}_t} V(r_s, \theta, \beta)^2 dS} = \frac{\int_0^{2\pi} \int_{\mathcal{D}_{\theta_{local}}} V(r_s, \theta, \beta)^2 \sin(\theta) d\theta d\beta}{\int_0^{2\pi} \int_0^\pi V(r_s, \theta, \beta)^2 \sin(\theta) d\theta d\beta}$$

where  $V(r_s, \theta, \beta)$  is the scalp voltage, as calculated using the four-region volume conduction model (see appendix), results in the local proportion of potential power,  $P_{local}$ , over a 15 degree radius of scalp (or a 30 degree diameter- about 4cm ).

### 2.4. EEG Experiments and Data Analysis

Fourteen subjects (12 males and 2 females) aged between 19 and 44 years, without a history of psychiatric or neurological disease, participated in this study after giving their written informed consent according to the standards of the CCNY Institutional Review Board. EEG experiments were performed in an electrically shielded, darkened room. Subjects were seated comfortably upright in a chair, or reclined in the prone or supine position (order counterbalanced among subjects) on a massage-bed with headrest. In the prone position, the forehead and cheeks rested on the donut-shaped massage pillow, while in the supine the head was supported by a neck pillow to avoid disturbing or putting pressure on the electrodes. Three computer monitors were matched for brightness and contrast using a luminance meter and situated in the corresponding centers of the visual field, and 11 inches distant to the eyes. EEG signals were recorded using a 128-electrode Active II system (BioSemi, Amsterdam, the Netherlands) at a 512Hz sampling rate.

Nine subjects took part in four EEG experiments modeled after classic visual paradigms from the literature: SSVEPs [41], Flash-VEPs [36], oddball ERP [11] and closed-eye alpha activity (see survey in [3]), to which the reader may refer for specifics. The amounts of stimuli were as follows: 10 groups of 10 seconds (alternating with 10 seconds of baseline) of checker reversal SSVEPs at 7Hz, 105 full-screen Flash-VEPs (in 5 groups of 21) at 0.7s apart, 32 oddballs out of 400 total stimuli (split into 5 blocks of 80), and 150 seconds of eyes open and eyes closed (in 5 sets of 30-second trials).

Fourteen subjects took part in the gamma activity experiment, which was modeled after the visual stimulus in an MEG study [21]. Between 288 and 432 seconds of baseline and ring stimulus (see Fig. 2), in which the rings moved out or in, were presented while the subject was instructed to fixate on the center dot. Baseline and stimulus were presented in blocks of 3 seconds each.

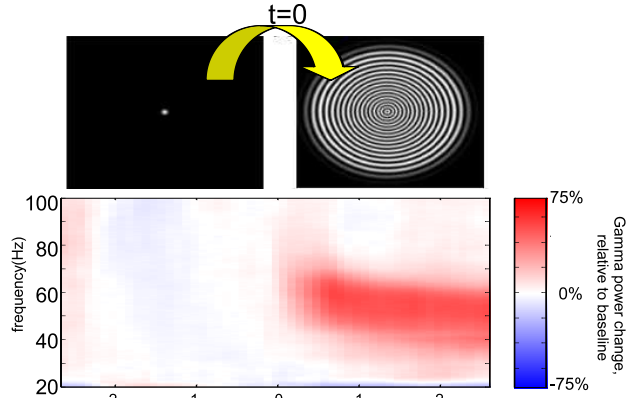


Figure 2: Spectrogram of one subject (S11) during baseline (dot) and 3 seconds of visual stimulus (moving rings), showing increase in activity over baseline, similar to results in [21].

For each subject and each paradigm, all three prone, supine, and sitting experiments were performed in the same session to keep the electrode position on the scalp as constant as possible. Total experiment time was roughly 4 hours per subject.

The data was first detrended and 60Hz and higher harmonic line noise was identified using Thompson’s F-test [47] and removed by sine-fitting and subtracting in 3 second windows, using the Matlab implementation in the Chronux toolbox [6]. The data was then reset to a common reference, and epoched. Data epochs contaminated by eye movements or muscle activity were manually rejected. For the alpha, gamma, and SSVEP data sets, in each epoch, a multi-Slepian taper spectral estimate was found and divided by the corresponding estimate of the corresponding baseline of the epoch. The oddball and Flash-VEP data was measured in microvolts then squared to get power.

The resulting data from the sitting experiments was then initially analyzed, from which times, frequencies, and regions of interest for each subject and each paradigm were determined (see Fig. 3). The resulting signal power (normalized by the baseline for alpha, gamma, and SSVEP data) was averaged over the individual’s region, time, and/or frequency band of interest (as determined from the sitting position) for that experimental paradigm, and compared within each subject using the Mann Whitney Wilcoxon rank sum test, corrected to have a False Discovery Rate [4] of less than 0.05. The signal powers were also averaged over all epochs for each subject, and a between position analysis was done using a paired sign test. All % changes are in terms of signal power (in  $\mu V^2$ ) and calculated as normalized by the mean:  $a$  and  $b$  are  $100 \frac{a-b}{\frac{1}{2}(a+b)}$  % different. For frequencies of interest that included 60Hz, the analysis was rerun while excluding the 60Hz frequency bin in order to confirm that the line-noise removal worked accurately and fairly.

### 3. Results

#### 3.1. Anatomical MRIs Show Brain Shift with Changing Position

An MRI study was performed to confirm reports in the literature [49] brain shift resulting from changing positions from prone to supine. All three subjects showed a statistically significant decrease in occipital CSF layer thickness from prone to supine, with changes of: subject CR:  $-27.64\%$ , ( $t(14) = -6.40, p = 1.65 \times 10^{-5}$ ), subject LCP:  $-19.22\%$ , ( $t(14) = -6.10, p = 2.8 \times 10^{-5}$ ), and subject JKR:  $-26.99\%$ , ( $t(14) = -8.91, p = 3.8 \times 10^{-7}$ ) respectively (averaged over the occipital pole, excluding the falx cerebri (see Methods)). As can be seen in Fig. 1, where we show the difference between the average prone and average supine SPMs, the largest changes in CSF thickness of approximately 30-40% were in the frontal and occipital poles. Given CSF thicknesses of about 3mm, we will hence adopt a convenient value of 1mm brain shift for the rest of this investigation.

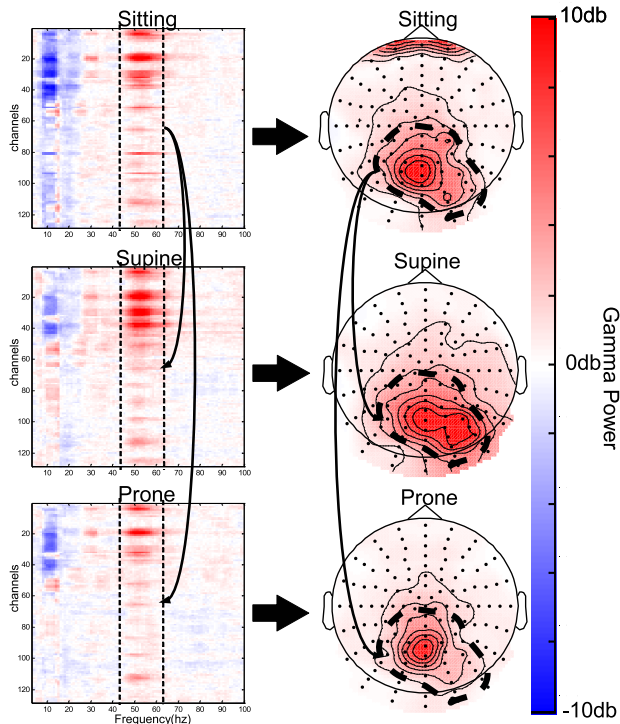


Figure 3: Method of determining frequency range and region of interest for one example subject (S6) in one paradigm (gamma activity). Frequency range of interest and anatomical region of interest are chosen from sitting data, and applied to prone and supine data.

### 3.2. Multi-Dipole Model Predicts Large EEG Magnitude Changes

The Multi-Dipole concentric head model results indicated that increasing the CSF thicknesses from 2mm and 3mm decreased the static estimated scalp potential by 16.7% for a single axially oriented dipole, and by 21.1% for a single tangentially oriented dipole (averaged over a 4cm neighborhood on the scalp), corresponding to 33.1% and 41.7% decreases in power.

For spatially dyssynchronous gamma activity, (assumed to originate in the calcarine sulcus [21], thus modeled using tangential dipoles), Monte-Carlo simulations of this model resulted in a prediction that the 1mm increase in CSF thickness would result in a larger decrease of 58.8% (see Fig. 4). In a similar simulation for the axial dipoles (representing the other, more conventional EEG paradigms), the power change did not increase because they were modeled as synchronous, and thus the amount of smearing had no net effect (see Discussion).

By rerunning the simulations with the CSF conductivity set equal to that of the gray matter, it was found that the corresponding brain shifts led to only a 14.3% and 35.2% decrease in respective power - indicating that a portion of the predicted effect can be attributed to simply moving the source (the brain) closer to the surface, while the rest is due to the higher conductivity of the CSF.

### 3.3. Prone to Supine Shift Selectively Enhances EEG Signals

To empirically measure the effect of the change in CSF thickness between prone and supine positions, four conventional EEG visual stimulus paradigms were implemented, namely, a checkerboard Steady-State Visual Evoked Potential(SSVEP) at 7Hz [41], a slow Flash-Visual Evoked Potential (FVEP) [36], an oddball Event Related Potential (ERP) [11] and closed-eye vs. open-eye alpha activity (see survey in [3]). A relatively new visually induced gamma paradigm was also included (see Fig. 2), taken from a recent MEG study [21].

For all of the classic EEG paradigms; FVEPs, SSVEPs, Closed-eye alpha, and oddball ERP, large magnitude signals (see Fig. 4) were found which were consistent in frequency, time, and space

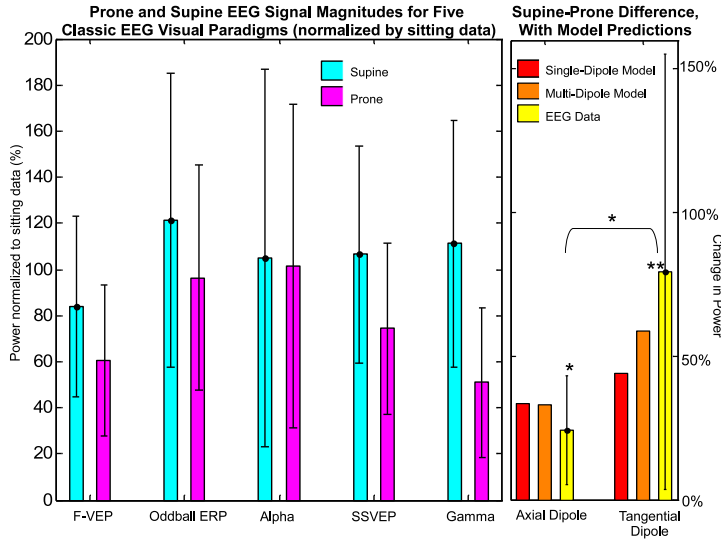


Figure 4: Left: Signal power for different testing stimuli and positions (bars represent 1 STD across subjects). Frequency data are shown as stimulus power relative to baseline, ERP data are shown as ( $\mu V^2$ ) to match. Right: differences between prone and supine signal power averaged across gamma (modeled as a tangential dipole), and all other stimuli (modeled as axial dipoles). Also shown are computational predictions. (\* $p < 0.05$ , \*\* $p < 0.005$ )

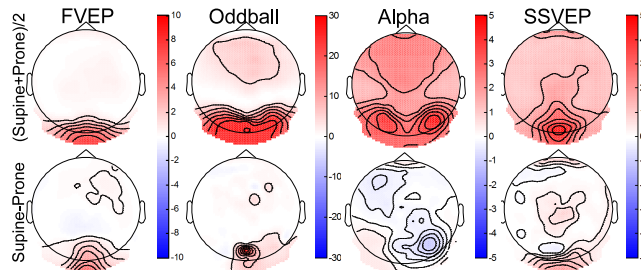


Figure 5: Grand average over all subjects and all trials. Top: average of prone and supine. Bottom: supine-prone. All data shown in power ( $\mu V^2$ ). )

between and within subjects, and matched well the canonical results in the literature (see Methods, Fig. 5). For all these stimuli, subjects' signal power increased from prone to supine: F-VEPs: 33.4%, oddball: 22.2%, Alpha 7.8%, SSVEP: 32.8%. While the sample number ( $N = 9$ ) was too small for each individual task to reach significance, the change is significant on average ( $t(8) = 3.81$ ,  $p = 0.0051$ ) and at 24.1% matches the sign and order of magnitude of the axial dipole prediction (the EEG scalp distributions evoked by these paradigms are consistent with axial dipoles). The standard deviation between sitting, prone, and supine positions was approximately half (47.7%) the size of the standard deviation between subjects for the four conventional stimuli, so the effect of position is quite large relative to the variability between subjects. Based on the shorter spatial coherence length of gamma generators in the brain, we expected that gamma activity would be more severely affected by the shunting of CSF, and thus would be more sensitive to changes in subject position. Indeed, the gamma variation with position was found to come from a different distribution than the other experiments ( $t(21) = 2.13$ ,  $p = 0.045$ ), and thus will be discussed separately (for a discussion of why this is the case, see section 4).

### 3.4. Gamma Activity Increased Greatly and Consistently

Persistent occipital gamma activity can be induced with moving concentric rings (see Fig. 2 and [21]). This visually induced gamma activity, as measured via EEG, was also of large magnitude and mostly consistent in terms of anatomical location (see Fig. 6) and frequency across subjects (e.g. some had activity in 40-55 Hz range, others in 60-70Hz range), and matched very well previous

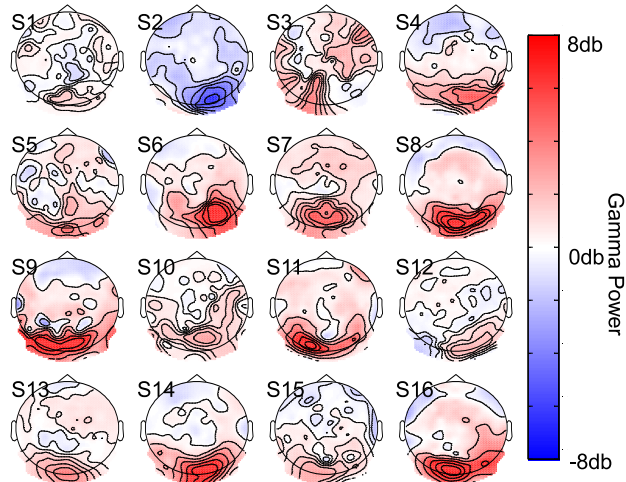


Figure 6: Difference between supine and prone gamma power in frequency band of interest. The occipital cortex of the non-significant subject (S12) did show increased gamma power, but it was not in the region of interest as defined by the sitting data (see Fig. 3). As for the paradoxical subject (S2), the gamma region of interest might have coincidentally been in a region in which the CSF changed thickness in the opposite direction (see Fig. 1), due to differing anatomy. Note that two subjects were each tested twice, months apart: S13=S7 and S16=S8, showing that the effect seems consistent in time.

MEG recordings [21] (see Fig. 2). Visual gamma activity is generally thought to be difficult to record using scalp EEG, and there is some discussion that transient gamma activity may result from mini-saccades [55]. However, this seems unlikely in this case due to the long-term sustained nature of the gamma activity (see Fig. 2).

Between the subjects, occipital gamma power from prone to supine changed by a proportionally much larger amount, 79.4% ( $t(13) = 3.92$ ,  $P = 0.002$ ), than the four conventional EEG paradigms (see Fig. 3 and Fig. 4). For individuals, this was a significant increase in 14 of 16 sessions (12 of 14 subjects) (False Discovery Rate  $q < 0.05$ ), indicating that the direction and significance is very consistent among subjects (see Fig. 6). The standard deviation between positions was greater than 75% the size of the standard deviation between subjects, so the effect of position is quite large relative to the variability between subjects. Although the size of the effect varied between individuals, the change has the correct direction and order of magnitude as the predictions by the simulations.

Note that when the 60Hz band was excluded from the analysis (to ensure that artifacts did not confound the results), the results were qualitatively the same: the same 12 subjects showed a significant increase in gamma power, and the overall average difference changed by less than 1 percent.

#### 4. Discussion

The brain ‘floats’ in a bath of CSF inside the skull, and when the head changes orientation relative to gravity, the brain shifts within the skull due to differences in density between brain tissue and CSF. This shift, as discussed in [58][29][49] and confirmed by the MRI data in this study, can cause up to a 30% change in thickness in the CSF layer between brain and skull when changing between prone and supine positions. While this approximately 1mm shift may seem minor in terms of the size of the brain, sizes of electrodes and their location precision, etc., CSF is up to 10 times more conductive than white or gray matter, and up to 100 times more conductive than bone [38][35], so changes in this thin layer of fluid actually lead to large changes in current flow, and hence scalp potential, as pointed out in the EEG forward-modeling and source-localization literature [39][38][51].

Semi-analytic calculations using a multi-sphere nonhomogeneous head model with a single static dipole, and parameters corresponding to the MRI data predict a shift from 3mm to 2mm of CSF thickness to correspond to an  $\approx 30-45\%$  increase in scalp power. However, when generalizing to multiple dynamic non-synchronized dipoles to more accurately model the gamma activity (see Methods), the results were an increase in power of 58.8%. These computational models, while based on a simple co concentric sphere model and hence not expected to be quantitatively precise, agree in direction and order of magnitude with the experimental results (see Fig. 4) using five EEG visual stimulus paradigms.

The great difference between the effect of CSF on power induced by the conventional (modeled by axial dipoles) and gamma (modeled by tangential dipoles) stimuli can be explained as follows. Studies have shown that while the other signals i.e. alpha, FVEPs, SSVEPs, and oddball ERP, are largely coherent in space, gamma activity is incoherent in space on a scale greater than 1cm [17]. The CSF in this case ‘smears’ the current, adding together neighboring signals, and decreasing the magnitude of local scalp potentials [37][14]. To investigate whether this might be the cause of this difference in experimental and simulation effect sizes, the distribution of the scalp potential  $V(r_s, \theta, \beta)$  (see formula 1 in appendix) as it varies with distance from the location directly over the electrode was calculated. In Fig. 7, one can see that the potential of the tangential dipole is much more spread out than the potential of the axial dipole, hence multiple tangential dipoles that are oscillating out of sync will interfere with each other more substantially than similarly positioned axial dipoles. In terms of power  $V^2$ , in the 30 degrees (corresponding to about 4cm on the scalp) nearest its peak, the potential power curve for the axial dipole contains 88.7% of the total weight of the curve, whereas the tangential has only 51.2%. Furthermore, this proportion changes much more with varying CSF for the tangential than for the axial dipoles. Integrating over the surface of the sphere (see Methods) shows that the change from 3mm to 2mm of CSF thickness increases the proportion of the power in a four cm neighborhood,  $P_{local}$ , by only 1.15% for the axial dipole, but 21.9% for the tangential dipole. Hence the point spread, and thus ‘smearing’ of tangential dipoles is affected much more by CSF thickness than that of axial dipoles, explaining why the gamma power, modeled by spatially incoherent tangential dipoles, was selectively increased in magnitude to such a large degree with decreasing CSF thickness.

While the changes in EEG signal power with position have been well explained by CSF thickness, it is also conceivable that such differences are due instead to actual changes in brain activity [45]. It is well known that changes in blood pressure between sitting and reclined positions can change brain activity via baroceptive signaling mediated by the locus coeruleus (see review in [26]), and this may account for some of the decrease in the measured results (see Fig. 4) from sitting to supine/prone (another factor that definitely contributes to this decrease is selection biases—the ROI’s and FOI’s were determined from the sitting data, see Fig. 3). However, this would not explain the difference between the prone and supine data itself, nor the fact that visually induced gamma activity was selectively enhanced so much more. Activation of the otolith system (which senses linear acceleration) might also have had an effect. While little work has been done on constant, immobile, postural effects on EEG (as is the case in this paper), 500Hz oscillation has been shown to have some effect on the visual cortex [30], and this idea should be further investigated.

Note that while it is tempting to try to interpret the alpha-activity results as being qualitatively different from those from the other stimuli based on the left side of Figure 4, actually, due to the small sample number ( $N = 9$ ), the results for the different stimuli are not significantly different from each other, and the results should only be interpreted as significant on average (see Results section 3.3). Nonetheless, a confounding increase of alpha activity in the reclined positions, due to a change in comfort or general arousal [10], might also have occurred. On the other hand, if the subjects remain engaged there is no reason to expect that alpha activity should increase, and we did not see any evidence of an increase in the prone/supine position relative to sitting. Similarly, evoked responses are known to be modulated by attention, which may vary during this lengthy experiment.

In summary, in this study it is shown that EEG power is indeed strongly affected by subject position (prone vs. supine), and the present data suggest that this is due to gravity induced changes in CSF layer thickness. As the precision of anatomically accurate models improve, concerns

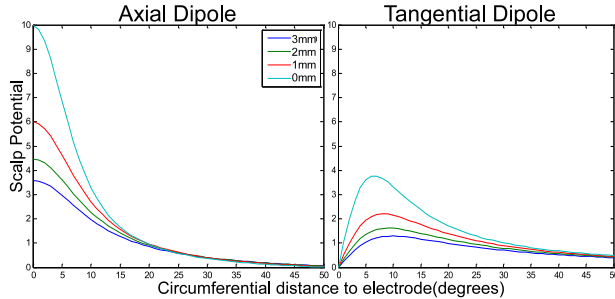


Figure 7: Scalp potential as a function of circumferential distance ( $\theta$ , in degrees) from axial and tangentially oriented dipoles, for different thicknesses of CSF.

expressed in [38] that head models generated from supine MRI scans may lead to errors in EEG source localizations may be warranted, an effect that might add to the confounding effect of “skin shift” [32]. Indeed, anatomically accurate models of current flows in the context of transcranial stimulation have shown that small errors in CSF thickness lead to significant changes in resulting current flows [13]. These results also provide another possible explanation for some of the effects of micro-gravity on EEG signals during space flight [8], and other EEG studies. For example, it is well known that EEG measured gamma power decreases with age [7] and certain neuro-degenerative diseases (e.g. Alzheimer’s) [20], however, the analysis in this paper shows that any such real decrease in internal gamma band power could be confounded by a thicker layer of CSF due to normal aging. Such an effect could also explain the increase in Electro-Convulsive-Therapy (ECT) thresholds with age, a widely reported phenomenon [9].

Additionally, many other diseases can cause moderate to severe brain atrophy and shrinkage, e.g. Traumatic Brain Injury (TBI) [28], hypoxia [18], multiple sclerosis [43], alcoholism, and carbon monoxide poisoning. The resulting thicker CSF layer, could greatly decrease EEG signals, as suggested by the present results. The sensitivity and specificity of EEG as a diagnostic tool for patients with such diseases (e.g. as a ‘confirmatory’ measure in diagnosing brain death [53]) should be investigated, since significant brain activity might not show up on an EEG due to this effect. Likewise, in light of these results, care should be taken when using EEG diagnostically on preterm neonates [50], since they have a thicker than normal CSF layer, and significant anterior brain shift has been noted in the literature [49].

The findings of this study can also have a benefit for a number of stimulation protocols, e.g. by optimally positioning subjects when performing transcranial direct current stimulation (tDCS)[33][13][15] or transcranial electrical stimulation (TES)[42]. The brain shift results alone could be useful for Transcranial Magnetic Stimulation (TMS), in which field strength drops off logarithmically [19] and a 1mm decrease in scalp-gray matter distance could be significant.

Beyond these implications, the central result of this paper is that subject position has a large and consistent effect on EEG signals due to brain shift. In the EEG experiments the standard deviation between positions was approximately half the size of the standard deviation between subjects for 4/5 of the stimuli, and more than 75% for the gamma activity. Thus, controlling head position in future studies could greatly decrease experimental variance. When possible, EEG subjects could also be oriented to minimize the thickness of the CSF layer over the location of interest, and thus maximize the signal to noise ratio. This holds especially true for weak, difficult to record, or spatially localized signals such as gamma activity, which is shown in this report to increase in measured power by an average of 79.4%, simply by switching position.

## 5. Appendix: Volume Conduction Model

To derive the simulation model, we will first make some simplifying assumptions. Given length scale  $L \approx 10\text{cm}$  and the shortest time scale  $\tau_g \approx \frac{1}{50\text{Hz}} = 0.02\text{s}$  (for gamma oscillations),  $\mu\sigma L^2 \approx 10^{-11}\text{s} \ll \tau_g$ , where  $\mu$  is the permeability (value for water used) and  $\sigma$  is the conductivity, a quasi-static approximation to the time varying Maxwell’s equations can be used [24]. Hence

Ampere’s law is reduced to  $\nabla \times H = J$ , and the divergence of each side yields  $\nabla \cdot J = 0$ , the continuity equation. Now applying Ohm’s law ( $J = \sigma E$ ) and the definition of the electric potential  $E = -\nabla V$ , results in  $\nabla \cdot (\sigma \nabla V) = 0$ , a Laplace equation.

Rewritten into spherical coordinates with azimuthal symmetry, this can be deconstructed via separation of variables:  $V(\theta, r) = \Omega(\theta)R(r)$ .  $\Omega(\theta)$  turns out to be equivalent to Legendre’s differential equation, and hence has solutions of Legendre polynomials  $P_n(\cos(\theta)) = P(x) = \frac{1}{2^n n!} \frac{d^n}{dx^n} [(x^2 - 1)^n]$ , while  $R(r)$  is a Frobenius equation, and can be solved using Frobenius’s method to get a solution of the form  $R(r) = Ar^{l+1} + Br^{-l}$ . This gives us the eigenfunctions, and generally a solution in terms of the spherical harmonics will have the form  $V(r_s, \theta) = \sum_{l=0}^{\infty} (A_l r_s^{l+1} + B_l r_s^{-l}) P_l(\cos(\theta))$  where  $A_l$  and  $B_l$  are determined by the boundary conditions, and  $r_s$  is the radius at the scalp surface (For a thorough derivation and background, see e.g. [24]).

A dipole, modeled as two equal and opposite monopoles, leads to a non-homogeneous Poisson’s equation  $\nabla \cdot (\sigma \nabla V) = I\delta(r - r_2) - I\delta(r - r_1)$  instead of the Laplace equation. The derivation and solution are thus more complicated, but come in a similar form:

$$V(r_s, \theta, \beta) = \sum_{n=1}^{\infty} f_n \cos(\alpha) P_n(\cos(\theta)) + g_n \cos(\beta) \sin(\alpha) P_n^1(\cos(\theta)) \quad (1)$$

and can be computed for the standard boundary conditions using the formulas in [56], where the coefficients of functions  $f_n$  and  $g_n$  are complicated relations of the thicknesses and conductivities of the various layers,  $\beta$  describes the angle between the dipole orientation and the measurement location, and  $\alpha$  describes the orientation of the dipole relative to the center ( $\alpha = 90$ : tangential,  $\alpha = 0$ : axial).

## 6. Acknowledgments

The authors thank all of the experimental subjects for their time, and Xiang Zhou and Dario Pinos for their assistance. This work was supported by DARPA Accelerated Learning Program, grant A10AP00051.

## References

- [1] Ashburner, J., 2007. A fast diffeomorphic image registration algorithm. *NeuroImage* 38, 95–113.
- [2] Ashburner, J., Friston, K. J., 2005. Unified segmentation. *NeuroImage* 26, 839–851.
- [3] Barry, R. J., Clarke, A. R., Johnstone, S. J., Magee, C. A., Rushby, J. A., 2007. EEG differences between eyes-closed and eyes-open resting conditions. *Clinical Neurophysiology* 118, 2765–2773.
- [4] Benjamini, Y., Hochberg, Y., 1995. Controlling the false discovery rate: A practical and powerful approach to multiple testing. *Journal of the Royal Statistical Society. Series B* 71, 289–300.
- [5] Blankertz, B., Tomioka, R., Lemm, S., Kawanabe, M., , Muller, K.-R., 2008. Optimizing spatial filters for robust EEG single-trial analysis. *IEEE Signal Processing Magazine* 25, 41–56.
- [6] Bokil, H., Andrews, P., Kulkarni, J. E., Mehta, S., Mitra, P. P., 2010. Chronux: A platform for analyzing neural signals. *Journal of Neuroscience Methods* 129, 146–151.
- [7] Bottger, D., Herrmann, C. S., von Cramon, D. Y., 2002. Amplitude differences of evoked alpha and gamma oscillations in two different age groups. *International Journal of Psychophysiology* 45, 245–251.

- [8] Cheron, G., Leroy, A., Saedeleer, C. D., Bengoetxea, A., Lipshits, M., Cebolla, A., Servais, L., Dan, B., Berthoz, A., McIntyr, J., 2006. Effect of gravity on human spontaneous 10-hz electroencephalographic oscillations during the arrest reaction. *Brain Research* 1121, 104–116.
- [9] Coffey, C. E., Lucke, J., Weiner, R. D., Krystal, A. D., Aque, M., 1995. Seizure threshold in electroconvulsive therapy: I. initial seizure threshold. *Biological Psychiatry* 37.10, 713–720.
- [10] Cole, R. J., 1989. Postural baroreflex stimuli may affect EEG arousal and sleep in humans. *Journal of Applied Physiology* 67, 2369–2375.
- [11] Courchesne, E., Hillyard, S. A., Galambos, R., 1975. Stimulus novelty, task relevance and the visual evoked potential in man. *Electroencephalography and Clinical Neurophysiology* 39, 131–143.
- [12] Curran, E. A., Stokes, M. J., 2003. Learning to control brain activity: A review of the production and control of EEG components for driving braincomputer interface (BCI) systems. *Brain and Cognition* 51, 326–336.
- [13] Datta, A., Bansal, V., Diaz, J., Patel, J., Reato, D., Bikson, M., 2009. Gyri-precise head model of transcranial direct current stimulation: Improved spatial focality using a ring electrode versus conventional rectangular pad. *Brain Stimulation* 2, 201–207.
- [14] DeLucchi, M., Garoutte, B., Aird, R. B., 1962. The scalp as an electroencephalographic averager. *Electroencephalography and Clinical Neurophysiology* 14, 191–196.
- [15] Dmochowski, J. P., Datta, A., Bikson, M., Su, Y., Parra, L. C., 2011. Optimized multi-electrode stimulation increases focality and intensity at target. *Journal of Neural Engineering* 8.
- [16] Dornhege, G., Blankertz, B., Curio, G., Mller, K.-R., 2004. Boosting bit rates in non-invasive EEG single-trial classifications by feature combination and multi-class paradigms. *IEEE Transactions on Biomedical Engineering* 51, 993–1002.
- [17] Freeman, W. J., Rogers, L. J., Holmes, M. D., Silbergeld, D. L., 2000. Spatial spectral analysis of human electrocorticograms including the alpha and gamma bands. *Journal of Neuroscience Methods* 95, 111–121.
- [18] Gale, S., Hopkins, R. O., 2004. Effects of hypoxia on the brain: Neuroimaging and neuropsychological findings following carbon monoxide poisoning and obstructive sleep apnea. *Journal of the International Neuropsychological Society* 10, 60–71.
- [19] George, M. S., Lisanby, S. H., Sackeim, H. A., 1999. Transcranial magnetic stimulation; applications in neuropsychiatry. *Archives of General Psychiatry* 55, 300–311.
- [20] Herrmann, C., Dermiralp, T., 2005. Human EEG gamma oscillations in neuropsychiatric disorders. *Clinical Neurophysiology* 116, 2719–2733.
- [21] Hoogenboom, N., Schoffelen, J.-M., Oostenveld, R., Parkes, L. M., Fries, P., 2006. Localizing human visual gamma-band activity in frequency, time, and space. *NeuroImage* 29, 764–773.
- [22] Hosek, R., Sances, A., Jodat, R. W., Larson, S. J., 1978. The contributions of intracerebral currents to the EEG and evoked potentials. *IEEE Transactions on Biomedical Engineering* 25, 405–413.
- [23] Hughes, J. R., 1996. A review of the usefulness of the standard EEG in psychiatry. *Clinical Electroencephalography* 27, 35–39.
- [24] Jackson, J. D., 1999. *Classical Electrodynamics*. John Wiley & Sons.

- [25] Jung, T.-P., Makeig, S., Stensmo, M., Sejnowski, T., 1997. Estimating alertness from the EEG power spectrum. *IEEE Transactions on Biomedical Engineering* 44, 60–69.
- [26] Lipnicki, D. M., 2009. Baroreceptor activity potentially facilitates cortical inhibition in zero gravity. *NeuroImage* 46, 10–11.
- [27] Lotte, F., Congedo, S. W. M., Lcuyer, A., Lamarche, F., Arnaldi, B., 2007. A review of classification algorithms for EEG-based braincomputer interfaces. *Journal of Neural Engineering* 4.
- [28] MacKenzie, J. D., Siddiqi, F., Babb, J. S., Bagley, L. J., Mannon, L. J., Sinson, G. P., Grossman, R. I., 2002. Brain atrophy in mild or moderate traumatic brain injury: A longitudinal quantitative analysis. *American Journal of Neuroradiology* 23, 1509–1515.
- [29] Maurer, C. R., Hill, D. L. G., Maciunas, R. J., Barwise, J. A., Fitzpatrick, J. M., Wang, M. Y., 1998. Measurement of intraoperative brain surface deformation under a craniotomy. *Neurosurgery* 43(3), 514–526.
- [30] McNERNEY, K., Lockwood, A., Coad, M., Wack, D., Burkard, R., 2011. Use of 64-channel electroencephalography to study neural otolith-evoked responses. *J Am Acad Audiol* 22(3), 143–155.
- [31] Millan, J. R., Renkens, F., Mourino, J., Gerstner, W., 2004. Noninvasive brain-actuated control of a mobile robot by human EEG. *IEEE Transactions on Biomedical Engineering* 51, 1026–1033.
- [32] Mitsui, T., Fujii, M., Tsuzaka, M., Hayashi, Y., Asahina, Y., Wakabayashi, T., 2011. Skin shift and its effect on navigation accuracy in image-guided neurosurgery. *Radiol Phys Technol* 4(1), 37–42.
- [33] Nitsche, M. A., Paulus, W., 2000. Excitability changes induced in the human motor cortex by weak transcranial direct current stimulation. *The Journal of Physiology* 527, 633–639.
- [34] Noback, C., Strominger, N. L., Demarest, R. J., Ruggiero, D. A., 2005. *The Human Nervous System*. Humana Press.
- [35] Oostendorp, T. F., Delbeke, J., Stegeman, D. F., 2000. The conductivity of the human skull: Results of in vivo and in vitro measurements. *IEEE Transactions on Biomedical Engineering* 47, 1487–1492.
- [36] Pascual-Marqui, R. D., Michel, C. M., Lehmann, D., 1994. Low resolution electromagnetic tomography: A new method for localizing electrical activity in the brain. *Psychophysiology* 18, 49–65.
- [37] Pfurtscheller, G., Cooper, R., 1975. Frequency dependence of the transmission of the EEG from cortex to scalp. *Electroencephalography and Clinical Neurophysiology* 38, 93–96.
- [38] Ramon, C., Schimpf, P., Haueisen, J., 2006. Influence of head models on EEG simulations and inverse source localizations. *BioMedical Engineering Online* 5.
- [39] Ramon, C., Schimpf, P., Haueisen, J., Holmes, M., Ishimaru, A., 2004. Role of soft bone, CSF and gray matter in EEG simulations. *BRAIN TOPOGRAPHY* 16, 245–248.
- [40] Rampil, I. J., 1998. A primer for EEG signal processing in anesthesia. *Anesthesiology* 89, 980–1002.
- [41] Regan, D., 1977. Steady-state evoked potentials. *Journal of the Optical Society of America* 67, 1475–1489.

- [42] Rothwell, J., Burke, D., Hicks, R., Stephen, J., Woodforth, I., Crawford, M., 1994. Transcranial electrical stimulation of the motor cortex in man: further evidence for the site of activation. *Journal of Physiology* 481, 243–250.
- [43] Rudick, R., Fisher, E., Lee, J.-C., Simon, J., Jacobs, L., 1999. Use of the brain parenchymal fraction to measure whole brain atrophy in relapsing-remitting ms. *Neurology* 53, 1698.
- [44] Salinsky, M., Kanter, R., Dasheiff, R. M., 1987. Effectiveness of multiple EEGs in supporting the diagnosis of epilepsy: An operational curve. *Epilepsia* 28, 331–334.
- [45] Schneider, S., Brmmer, V., Carnahan, H., Dubrowski, A., Askew, C. D., Strder, H. K., 2008. What happens to the brain in weightlessness? a first approach by EEG tomography. *NeuroImage* 42, 1316–1323.
- [46] Teplan, M., 2002. Fundamentals of EEG measurement. *Measurement Science Review* 2, 1–18.
- [47] Thomson, D. J., 1982. Spectrum estimation and harmonic analysis. *Proceedings of the IEEE* 70, 1055–1096.
- [48] Tomioka, R., Mller, K.-R., 2010. A regularized discriminative framework for EEG analysis with application to braincomputer interface. *NeuroImage* 49, 415–432.
- [49] Wallois, F., Mahmoudzadeh, M., Patil, A., Grebe, R., 2011. Usefulness of simultaneous eeg-nirs recording in language studies. *Brain and Language in Press*.
- [50] Watanabe, K., Hayakawa, F., Okumura, A., 1999. Neonatal eeg: a powerful tool in the assessment of brain damage in preterm infants. *Brain and Development* 21(6), 361–372.
- [51] Wendel, K., Narra, N. G., Hannula, M., Kauppinen, P., Malmivuo, J., 2008. The influence of CSF on EEG sensitivity distributions of multilayered head models. *IEEE Transactions on Biomedical Engineering* 55, 1454–1456.
- [52] Wiesera, H. G., Schindlera, K., Zumstegb, D., 2006. EEG in CreutzfeldtJakob disease. *Clinical Neurophysiology* 117, 935–951.
- [53] Wijdicks, E., 2001. The diagnosis of brain death. *The New England Journal of Medicine* 334, 1215–1221.
- [54] Wu, W., Gao, X., Hong, B., Gao, S., 2008. Classifying single-trial EEG during motor imagery by iterative spatio-spectral patterns learning (ISSPL). *IEEE Transactions on Biomedical Engineering* 55, 1733–1743.
- [55] Yuval-Greenberg, S., Tomer, O., Keren, A. S., Nelken, I., Deouell, L. Y., 2008. Transient induced gamma-band response in EEG as a manifestation of miniature saccades. *Neuron* 58, 429–441.
- [56] Zhang, Z., 1995. A fast method to compute surface potentials generated by dipoles within multilayer anisotropic spheres. *Physics in Medicine and Biology* 40, 335–349.
- [57] Zhou, H., van Oosterom, A., 1992. Computation of the potential distribution in a four-layer anisotropic concentric spherical volume conductor. *IEEE Transactions on Biomedical Engineering* 39, 154–158.
- [58] Zhu, Q., Dougherty, L., Margulies, S. S., 2003. In vivo measurements of human brain displacement. *Summer Bioengineering Conference, Key Biscayne, Florida*.